IEEE Open Access Journal of
Power and Energy

Received 3 June 2019; revised 19 August 2019; accepted 15 October 2019. Date of publication 11 November 2019;
date of current version 2 January 2020.

Digital Object Identifier 10.1109/OAJPE.2019.2952812

A Benchmark Distribution System for Investigation of Residential Microgrids With Multiple Local Generation and Storage Devices

SYED A. RAZA (Student Member, IEEE), AND JIN JIANG (Fellow, IEEE)

Department of Electrical and Computer Engineering, The University of Western Ontario, London, ON N6A 5B9, Canada

CORRESPONDING AUTHOR: J. JIANG (jjiang@eng.uwo.ca)

This work was supported by NSERC Discovery Grants Program under Grant RGPIN-2018-05654.

ABSTRACT A benchmark distribution system is developed for investigating control and energy management of distributed generation (DG) at a residential level in the form of three single-phase microgrids. The benchmark is derived from a typical distribution network architecture with common parameters found in North-America systems including wiring specifications, line impedances and connection details for rooftop PV systems. This benchmark system can accommodate microgrids operating in both grid-connected and islanded modes. Within this benchmark, multiple single-phase DG sources located in different phases can be coordinated to form a dynamically balanced three phase system under different load and generation profiles in different phases. The coordination of DG sources in a particular phase is achieved through an intra-phase power management device, while mitigating loads and generation imbalance among all phases are done by an inter-phase power management scheme. It is expected that this benchmark system will facilitate investigation of impacts posed by proliferation of single-phase distributed generation devices and local storage systems in private residences. Three case studies have been carried out to demonstrate the versatility and effectiveness of this benchmark system.

INDEX TERMS Residential microgrids, single-phase systems, cooperative control, back-to-back converters, benchmark distribution system.

I. INTRODUCTION

AS PROLIFERATION of roof-top PV systems and household energy storage units at residential setting continues, the landscape of distribution systems is changing rapidly [1]. A modern distribution system in a residential neighborhood has to be able to accommodate multiple embedded generation and energy storage units [2], [3] in both single- or three-phase configurations. In fact, these local generation and storage capacities allow a group of such devices to be connected together to form a single- or three-phase microgrid to supply local loads. Such systems can operate in either a grid-connected or an islanded modes [4], [5]. This rapidly evolving trend has forced local utility companies to carry out extensive planning, load-forecasting, for both steady state and dynamic capacity studies, and reliability assessment of their distribution system infrastructure [6]. Needless to say, to carry out such studies, it is imperative to have a more detailed realistic model to capture ever-changing landscape in distribution systems.

Even though the subject of distribution systems is well-studied, however, most are focusing on steady state analysis and network reconfiguration in a multi-bus environment [7]–[9]. Since distributed generation is dynamic in nature, often affected by environmental conditions, power management and control studies have to consider transient behaviors of the system at a low voltage (LV) residential settings. Often, a family-owned roof-top PV systems and battery-based storage units are connected to form a residential microgrid connecting to a primary feeder on a single phase. In this respect, it is not only important, but also necessary to have a generic distribution network configuration, which can cope with various studies for residential microgrids.

Even though many microgrids have been developed to work at a distribution level in the literature, few can be

directly used for residential applications. Literature on such subject is very scarce. A distribution network is introduced in [10] to study an adaptive critic-based approach for grid-connected microgrids. It consists of a single point of common coupling (PCC) with multiple three-phase feeders from a local substation. The microgrid contains several DG units and three-phase loads aggregated as the secondary feeder loads. With the provision of local generation at a customer end, the need to accommodate details of local distribution transformers and customer loads becomes an integral part of the system model requirements. Even though the distribution network used in that study is capable of coordinating DG units in a three-phase microgrid environment, it does not have any capability to coordinate multiple single-phase units in the form of residential microgrids.

In other studies, microgrids are connected directly to the main grid without due consideration of transformer interface at substations, nor reactance associated with feeders [11]–[13]. For example, transitions of a three-phase microgrid from an islanded to a grid-connected modes have been investigated in [11] with focus on synchronization procedures. The associated distribution system has been simplified with a direct connection to the grid at the PCC. Furthermore, only aggregated constant resistive loads are considered.

The microgrid considered in [12] consists of three power electronics-interfaced DG units connected to an IEEE 5-bus system. The IEEE x-bus standards (where $x < 13$) are typically used, where key features of a LV distribution networks are omitted for simplicity in analysis. As a result, this model does not contain sufficient detail to meet the needs in residential microgrid studies, where one of the key points is coordination of multiple DG units using different power management strategies at a customer level.

The microgrid explored in [13] is composed of a multi-bus system with renewable energy sources connected to individual buses. The system architecture allows for aggregated loads at the feeders and interconnection among the studied microgrid, the utility network, and at individual buses serving local loads without due consideration of transformers or interfacing devices. Furthermore, the renewable energy sources are assumed to operate as centralized units on a bus, rather than being distributed as in realistic residential microgrids. Hence, this architecture does not represent a realistic distribution system in residential microgrids with generation sources and storage devices located at different phases.

Residential microgrids have been investigated in [14]–[16]. A laboratory-scaled single-phase radial microgrid is considered in [14] with generators and loads connected to local nodes. The architecture is more suited for three-phase microgrids with small micro-turbines as DG sources that serve a residential community. No coordination among DG sources has been considered. Furthermore, some of the losses in key system components, such as distribution transformers, have not been taken into account. This network architecture would not provide an effective framework for residential microgrid related studies.

A hybrid PV/battery system for a single household is examined in [15]. A PV/battery system and local loads are connected to a household distribution panel only. However, the distribution system topology, primary feeder and transformers have not been considered, nor on potential coordination with DG units nearby, such as devices from next door neighbors on the same local distribution network.

An energy management strategy has been considered for a grid-connected residential microgrid in [16]. The system consists of multiple DG sources connected to a three-phase network at the PCC. The local and central energy management systems allow for coordination of local generation and storage in residential units to achieve a state-of-charge (SOC) equalization. This would avoid prolonged load shedding for some customers under an islanded condition in case of insufficient supply. For this coordination strategy to work, the customers need to be on the same phase as the primary feeder. In a residential microgrid, different customers could be fed from different phases on a same primary feeder. Consequently, such system architecture and associated control strategies are not suitable for realistic situations in a practical distribution system.

An islanded hybrid single- and three-phase microgrid has been considered in [17]. This single-phase microgrid has DG units with local loads on two of the phases while the third phase is dedicated to loads only. Only single-phase loads have been considered. Despite of this unique feature, this architecture cannot be adopted where single-phase sources and loads are located in all three phases. Furthermore, the control objectives are based on unidirectional power flow between phases, they are not suited for power sharing studies in residential microgrids among different phases, where the power flow among phases can be bi-directional. The actual direction and the amount of power transfer depend on the availability of surplus power and power mismatch among phases.

To investigate control and power management issues for single- and three-phase microgrids with individual DG sources, storage devices, and loads in different phases, it is imperative to develop a benchmark model with versatile, yet flexible, architectures. Since structure and parameters of distribution systems are country and region specific, the current work will focus on those commonly found in North America.

The developed benchmark model is flexible enough to simulate a section of a distribution system by considering details of feeder reactance, different transformer configurations and wiring conventions of residential loads including roof-top PV systems and battery storage devices in the laterals of a primary feeder. This feeder can also supply power to common three-phase loads; say, a school, or a local community center. As compared to those in the literature, the current benchmark model is more realistic to a practical distribution system environment. In an islanded operating mode, the benchmark has the capability of exchanging power among phases through a

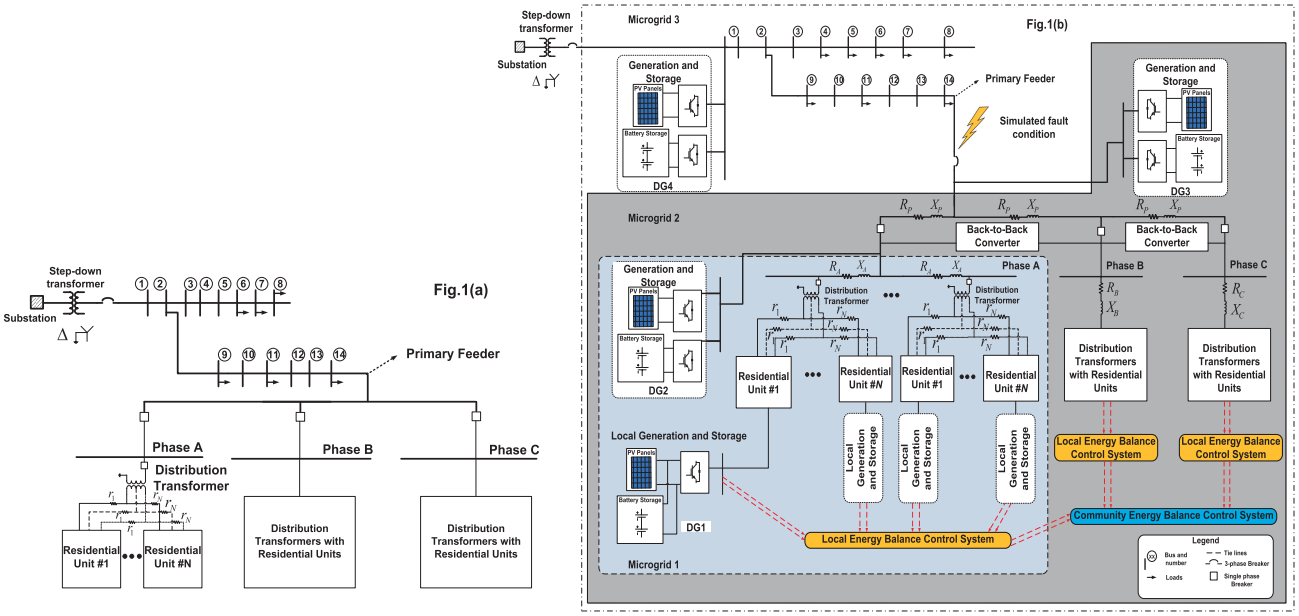

FIGURE 1. (a) A simple radial distribution system with residential units. (b) A radial distribution system with DG and storage devices in a form of residential microgrids.

power management unit based on a back-to-back converter configuration.

The paper is organized as follows; an overview of the existing distribution network in North America is explained in Section II. Section III identifies potential limitations of existing distribution network models in light of proliferation of residential size DG and battery storage devices. To address these limitations, in Section IV, a benchmark distribution system architecture is developed. Using this benchmark, detailed studies of a residential microgrid have been carried out in Section V. Section VI presents the simulation results of three case studies performed in PSCAD/EMTDC followed by the conclusion.

II. DISTRIBUTION NETWORKS IN NORTH AMERICA

A simple radial distribution system from the local substation to customers with residential loads is illustrated in Fig.1(a) while the same network with DG units is shown in Fig.1(b). In Fig.1(b), the PV and storage units are assumed to be located at customers' houses. These units can also be either central to the phase, primary feeder or to the distribution network. The back-to-back converters interconnect the three phases for potential power transfer. The key features of a distribution network are discussed in this section. For the sake of simplicity, residential loads connected to bus#14 only are shown here.

A. LOCAL SUBSTATION TO LOCAL DISTRIBUTION TRANSFORMER

Even though the topology from bulk power sources to a distribution network can vary from a simple radial system to more complex network configurations, the primary feeders still serve a locality or a geographical area near the local substation. As shown in Fig.1(a) the primary feeder can branch out into several circuits or laterals. These laterals can be in a single-phase form and sub-laterals may be tapped out subsequently, if necessary. These laterals can be located in residential or rural areas, and normally consist of a single-phase conductor and a neutral. Larger loads, such as those of schools, community centers, local industrial sites may be served by either dedicated underground or overhead primary feeders. They are mainly in three-phase.

B. LOCAL DISTRIBUTION TRANSFORMER TO CUSTOMERS

Each phase in a primary feeder serves a group of residential units. A split single-phase pole transformer is often used to step down the voltage even further to meet the voltage level for residential, commercial and industrial users as shown in Fig.2. Such split phase transformers are available in both 120 V and 240 V with a common neutral to customers. The local transformer steps down the feeder voltage from 13.8 kV to 120 V/240 V [18].

C. AT CUSTOMER'S END

The voltages of the power source at a customer site can be either 120 V or 240 V from outlets routed from a local split phase transformer. These dual voltage outputs are obtained conveniently between a phase and the ground (120V), or between two phases (240 V). A single line diagram showing such layouts is highlighted in Fig.2.

D. PV CONNECTION AT RESIDENTIAL UNITS

At residential sites, customers can set-up their own PV units to off-set their household consumption or export to the grid. A single line diagram of a typical PV connection at a res-

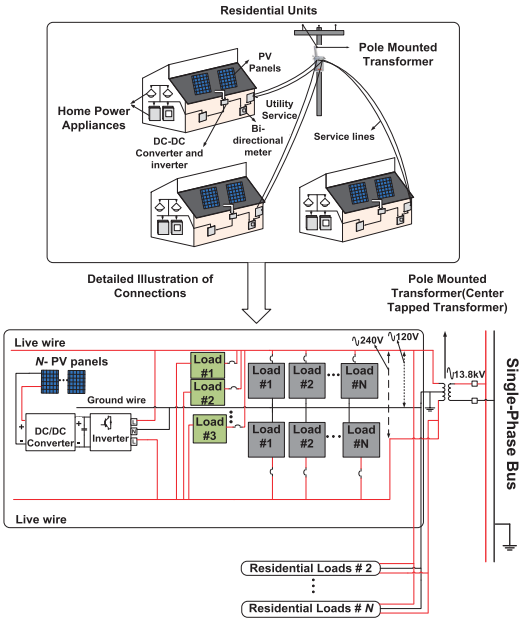

FIGURE 2. **A per-phase diagram from a distribution transformer to customers.**

idential site is shown in Fig.2. After the converter stage, the PV inverter output can be connected to the primary panel board through an AC disconnect switch. As depicted in Fig.2, the primary panel board is connected to a bidirectional utility meter, which measures the net energy usage for accounting purposes.

III. LIMITATIONS IN EXISTING DISTRIBUTION NETWORK MODELS FOR RESIDENTIAL MICROGRID STUDIES

The existing models of the distribution network are not meant for dealing with newly introduced DGs for microgrid studies. Installation of high number of DG units, as shown in Fig.1(b), requires enhancements to existing distribution network models. In essence, the following limitations have been identified for the existing distribution network models:

1) Most of the microgrid studies in the literature (as discussed in Section I) tend to focus on three-phase systems. With proliferation of singe-phase PV systems, battery storage units, and large short-term loads (e.g. electric cars) at residential levels, there is a need for a benchmark distribution network model, which can be used to investigate the effects of these non-traditional devices on the distribution networks. As reported in [19], with high PV proliferation, the peak PV generation can become twice the capacity of the local transformer. As a result, this can have a negative impact in the overall balance of the grid system;
2) With installation of phase-wise generation and storage units, single-phase microgrids can be formed on individual phases. The existing distribution network models do not support such single-phase configuration scenarios for coordination control and energy management within each phase and between two different phases. This is mainly because of the imbalance that is created, due to the difference in generation and load demand. Previous works in unbalanced conditions at the microgrid level have been focused on harmonic current injection at the DC link to compensate the non-linear loads [22]–[28]. These studies are limited to centralized PV generation and storage in three-phase;
3) To the best of our knowledge, the problem addressed herein poses a unique challenge to the current distribution systems, whereby there exist no distribution system models in the literature that can accommodate realistic situations of phase-wise generation and storage while simultaneously coordinating the multiple singe-phase DG units installed in different phase(s) and then connected on to a three-phase primary feeder;
4) The network model with its coordination control strategy should ensure that the voltage and frequency in each phase are maintained by balancing generation and consumptions under different conditions in that particular phase, while trying as much as possible towards balancing the three phases. This feature is not supported in the existing distribution system models;
5) Community based power sharing using controllable power electronic devices is a novel idea for single-phase microgrids, as studied in [20], [21]. Currently, there is no standard distribution system model that can provide a unified framework to investigate power and load sharing among different microgrids in separate phases;
6) At present, the system utilized by distribution utilities can give the operators real time visualization of current state of the network, fault zones or regions under maintenance etc. The proposed system is a step towards deployment of these residential microgrids whereby, the system operators can simulate their jurisdiction's network off-line. This will later help them to later deploy such microgrids in the future; and

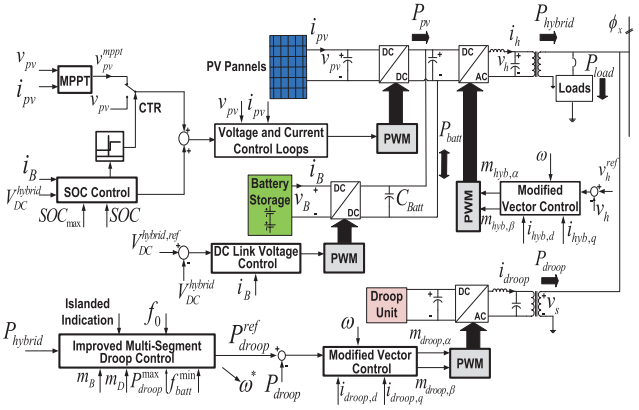

FIGURE 3. **The developed intra-phase control scheme [20], [21].**

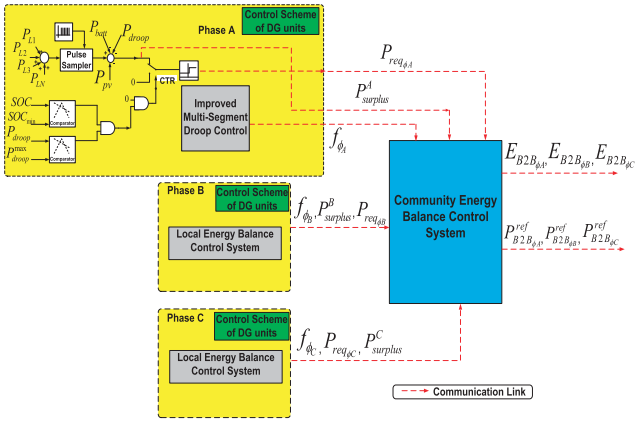

FIGURE 4. Coordination of network controller for single-phase microgrids using communication links.

7) By making use of the proposed benchmark distribution network with its various configuration parameters, the ratings of back-to-back converters, the potential system unbalance with multiple DG sources and the control parameters can be determined.

IV. SINGLE-PHASE RESIDENTIAL MICROGRID STUDIES

The developed benchmark model overcomes the identified deficiencies in the existing distribution system models as in Section III. This new benchmark model is capable of supporting ever-increasing number of DG units introduced at individual consumer sites. Without loss of generality, three regions of interest are highlighted in Fig.1:

1) At the left corner of Fig.1, a set of local PV generation and storage units has been referred to as DG1. The generation and storage that are located centrally with respect to phase A, is referred to as DG2. It serves the customers that are connected to this phase through multiple distribution transformers. PV/storage at each residence (DG1) can be used together with central generation (DG2) to form Microgrid # 1. This configuration can be repeated in phase B and/or phase C.
2) Microgrid # 2 overlaps some region of Microgrid # 1 as is evident from Fig.1. Microgrid # 2, referred to as DG3 in Fig.1, has its generation and storage installed on the primary feeder at bus#14, which is central to its three phases. If a fault occurs on bus#14, the loads on this feeder can be served through this architecture.
3) Finally, DG4 serves the distribution system from the substation onwards. The PV generation and storage units are placed next to the first serving bus. It can serve as a temporary source, should a fault occurs in the substation or on the incoming transmission line. The location of DG4 is strategic with respect to the entire distribution network under the current consideration. With DG4, Microgrid # 3 has been formed, which incorporates both Microgrids # 1 and # 2 within its jurisdiction.

TABLE 1. Operating conditions and control objectives for residential microgrids

Sr#	Operational Scenarios	Control Objectives
Intra-phase Power Management		
I.	• Loading and Generation: $P_{load}\|_{\phi_x} < P_{pv}\|_{\phi_x}$ • System Frequency: $f_0 < f < f_0 + \Delta f_{max}$ • Battery's health: $SOC_{min} \leq SOC \leq SOC_{max}$ or $SOC \rightarrow SOC_{min}$	• Only PV unit handles load. • The battery charges using the CIEMAT charging model, eq.(A.1) [29]. • The droop unit does not share power. • The improved multi-segment droop strategy follows Zone A as in [20], [21].
II.	• Loading and Generation: $P_{load}\|_{\phi_x} = P_{pv}\|_{\phi_x}$ • System Frequency: $f = f_0$ • Battery's health: $SOC_{min} \leq SOC \leq SOC_{max}$	• Only PV unit handles load. • The battery operates in floating state. • The droop unit is not required. • The improved multi-segment droop strategy again follows Zone A as in [20], [21].
III.	• Loading and Generation: $P_{pv}^{mppt}\|_{\phi_x} < P_{load}\|_{\phi_x} \leq P_{batt}^{max}\|_{\phi_x}$ • System Frequency: $f_{batt} < f < f_0$ • Battery's health: $SOC_{min} \leq SOC \leq SOC_{max}$	• The hybrid unit consisting of both PV and battery share the load. • The battery discharges using the CIEMAT discharge model, eq.(A.3) [29]. • The droop unit is not required. • The improved multi-segment droop strategy again follows Zone B as in [20], [21].
IV.	• Loading and Generation: $\left(P_{pv}^{mppt} + P_{batt}^{max}\right)\|_{\phi_x} < P_{load}\|_{\phi_x} \leq P_{droop}^{max}\|_{\phi_x}$ • System Frequency: $f_{batt}^{min} < f < f_{min}$ • Battery's health: $SOC_{min} \leq SOC \leq SOC_{max}$	• The hybrid and droop units share load. • The battery discharges using the CIEMAT discharge model, eq.(A.3) [29]. • The battery power is limited by the SOC control at P_{batt}^{max} as shown in Fig.3. • The improved multi-segment droop strategy again follows Zone C as in [20], [21].
Intra- and Inter-phase Power Management		
V.	• Loading and Generation: $P_{load}\|_{\phi_x} > (P_{pv}^{mppt} + P_{batt}^{max} + P_{droop}^{max})\|_{\phi_x}$ • System Frequency: f_{min} • Battery's health: $SOC_{min} \leq SOC \leq SOC_{max}$	• The hybrid and droop units share load. • The battery discharges using the CIEMAT discharge model, eq.(A.3) [29]. • The battery power is limited by the SOC control at P_{batt}^{max} as shown in Fig.3. • The 'Community Energy Balance Controller' decides the contributing phase for power sharing between the power surplus phase and the power deficient phase. • The control signals for the relevant back-to-back converter are enabled. • The power transferred through the back-to-back converter is given by, $P_{B2B}^{ref} = P_{hybrid} - P_{pv}^{mppt} - P_{batt}^{max}$ • The improved multi-segment droop strategy again follows Zone D as in [20], [21].

Some of the salient features of this developed benchmark distribution network model are discussed next.

A. COORDINATION OF DG UNITS IN GRID CONNECTED MODE

The developed benchmark distribution system can be used to study various scenarios in grid-connected residential microgrids. These may involve the coordination of several microgrid structures within a distribution network. Due to the presence of phase-wise generation and storage units, the benchmark allows for some of the local loads to be supported by the grid, while others by the local PV/battery hybrid

systems. This segregation of supplies for loads between the utility and local DG sources is usually dependent upon a specific configuration of connection and accounting arrangements of a customer [30].

B. COORDINATION OF DG UNITS IN AN ISLANDED MODE

For islanded residential microgrids, coordination of DG units is more complex as compared to that in grid-connected systems, because one can no longer use the grid as the reference for voltage and frequency regulation. The situation becomes even more complicated when single-phase DGs and loads are considered. By referring to the structure for residential microgrids in Fig.1, the following control and coordination issues should be investigated:

1) In Microgrid #1, the DG1 at each customer's home, needs to be coordinated with DG2. Control strategies can take this task on by either a master-slave or a multi-master arrangement. If a master-slave approach is chosen, DG2 can be designated as the 'master unit' to regulate the voltage and frequency in Microgrid # 1, while the DG1 will be run as a slave unit. These units will be operated as power controlled sources. In a multi-master configuration, two or more identified DG units can be used to regulate the frequency and the voltage profile in Microgrid # 1. This can be achieved if the units are arranged in droop controlled modes. Since it is necessary to maintain local power management within a phase, such schemes are referred to as intra-phase power management. Detailed coverage of a modified vector control and improved multi-segment droop control scheme adopted for the intra-phase power management module can be founded in [20], [21]. A block diagram representation is shown in Fig.3. Five representative power management scenarios and their respective control objectives are tabulated in Table 1. These scenarios have been considered in the case studies as described in Section VI to demonstrate the working principles and effectiveness of the proposed intra-phase power management strategy.
2) The system originated from the primary feeder has been designated as Microgrid # 2 as shown in Fig.1. Even though this microgrid contains three phases, they are made up by a single-phase microgrid with nested DG units. The control strategy allows individual phases to share power under an islanded condition according to their load demands, capacities of DG units and the state of charge of the battery storage units. In this way, it is possible to achieve a balanced three-phase system even through each phase can have very different local characteristics. This is achieved by the inter-phase power management scheme, known as 'Community Energy Balance Control System' as shown in Fig.4.
3) Since Microgrid # 2 is connected with Microgrid # 1, DG 3 in Microgrid # 2 will have to be coordinated with DG 1 and DG 2 in Microgrid # 1 as well. By a similar token, Microgrid # 3 will also need to be coordinated with Microgrids # 1 and # 2. Such nested configuration makes control and power management challenging, but at the same time, makes this model more versatile to adapt to various realistic system configurations.

TABLE 2. Parameters of a step down transformer at a local substation

Transformer type	$\Delta - Y$
Primary winding (L-L RMS)	69 kV
Secondary winding (L-L RMS)	13.8 kV
3-ϕ transformer (MVA)	100 MVA
Operating frequency	60 Hz
Positive sequence leakage reactance	0.0675 p.u
Air core reactance	0.2 p.u
Knee voltage	1.17 p.u
Magnetizing current	2%

TABLE 3. Parameters of a primary feeder

Length of primary feeder	8 km
Height of pole	30 m
Horizontal spacing between conductors	1 m
Vertical offset of central conductor	0.5 m
Shunt conductance	$1x10^{-11}$ mho/m
Resistivity	1 ohm*m
Resistance of conductor (R_p)	2.311 $m\Omega/100ft$
Reactance of conductor (X_p)	3.314 $mH/100ft$

V. BENCHMARK DISTRIBUTION SYSTEM MODEL FOR RESIDENTIAL MICROGRIDS

A section of radial distribution network of Fig.1 from the local substation to customer residences, as shown in Fig.2, is used as an example in the following analysis. The voltage from the substation has been stepped down from 69 kV to 13.8 kV in the current study. The parameters adopted for the substation step down transformer are presented in Table II [31].

The primary feeder adopted in this model corresponds to an overhead three-phase transmission line, supported by utility poles with the length varying between 1.61 and 24 km. According to ABB, the reactance (R_p and X_p shown in Fig.1) of a 1000 kcm primary feeder cable, are given in $m\Omega/100ft$ [32]. For a 13.8 kV primary feeder, the parameters, including the values of the reactance used are tabulated in Table III.

VI. CASE STUDIES

To validate performance of the benchmark distribution system, the architecture of Microgrid # 1, as shown in Fig.1, is used for both grid-connected and islanded scenarios of residential microgrids. The configuration parameters of various elements of the model are discussed first followed by the simulation scenarios. It is assumed that one of the primary feeders from the local substation is equipped with a hybrid PV/battery unit and a droop controlled unit in each phase, with interconnecting back-to-back converters to form a residential microgrid. A solution time step of $0.5\mu s$ is used in the simulations using PSCAD/EMTDC.

TABLE 4. Parameters of a local distribution transformer

Transformer type	Central tapped
Primary winding (L-L RMS)	13.8 kV
Secondary winding (L-L RMS)	120/240 V
Transformer (MVA)	0.075 MVA
Operating frequency	60 Hz
Positive sequence leakage reactance	0.02 p.u
No load losses	0.0075 p.u
Air core reactance	0.2 p.u
Knee voltage	1.17 p.u
Magnetizing current	1%

A. CONFIGURATION PARAMETERS OF THE BENCHMARK DISTRIBUTION NETWORK

The local distribution transformer used is a centrally tapped transformer, which further steps the voltage down from 13.8 kV to 120/240 V. The parameters of a local distribution transformer used in the model are summarized in Table IV [31]. In this study, 10 residential units have been assigned to one phase from the primary feeder. It is assumed that all the houses covered by the phase are situated at a distance of 10 m from each other. This distance will add to the resistance of electric cables, that are laid for each unit.

Typically 1/0 Aluminum-Copper Steel Reinforced (ACSR) cable is used for underground service connections to residential units. In older communities, overhead connections are still used. In these cases, the parameters may need to be adjusted. The values for the cable resistance in each phase are denoted by r_1 and r_N, where N represents the total number of houses served on a phase as shown in Fig.1. The resistance of 1/0 ACSR cable is $5.22 \times 10^{-4}\Omega/m$ [33]. Assume that the maximum permissible voltage drop in the service cable from the transformer to the Nth house is 2% [18], [31], then, the maximum drop in voltage can be calculated as $V_D = 120 \times 2\% = 2.4V$. The power panel boards at each house are commonly rated at 100 A [34]. Therefore, the resistance of the service cable can be derived as $\Delta r_N = 2.4V/100A = 0.024\Omega$. This is nearly equivalent to $45m$ of additional service cable for the 10th house, as compared with that of the house nearest to the distribution transformer. Additional cable may even be required for overhead clearance [34].

The local distribution transformer and residential units on phase A of the primary feeder can be repeated for the other two phases, given that the loading in each phase is similar. Otherwise, transformers with different MVA ratings need to be used as per regulations.

As shown in Fig.1, the three-phase primary feeder is routed to serve local residential units. For a typical #4 AWG cable, the reactance represented by R_A and X_A in Fig.1 is taken as $27.4 + j10.45m\Omega/100ft$ [33]. The advantage of using these parameters in the model can become clear when single-phase laterals are loaded with multiple groups of residential units, which are separated by some distance. The reactance will cause voltage drops along the lateral. The amount of such voltage drops will depend on actual loading of the residence, quality of the cable used and the number of homes served by the primary feeder.

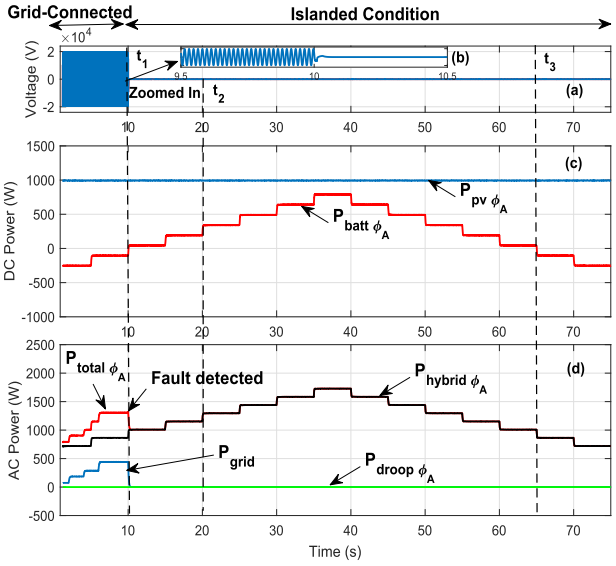

FIGURE 5. Voltage and power variations during a transition from a grid-connected to an islanded mode using the benchmark distribution system model.

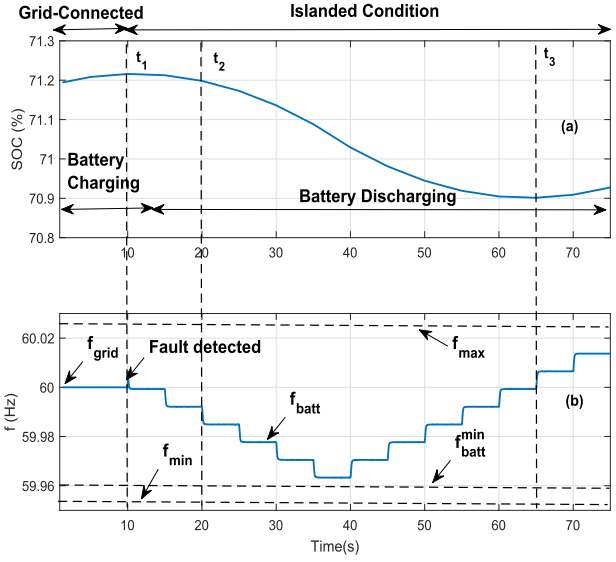

FIGURE 6. Variations in the SOC and the system frequency at the transitions from a grid-connected to an islanded mode using the benchmark distribution system model.

The residential units in Fig.1 have the same electrical layout as shown in Fig.2. Each unit is assumed to have some typical household electrical apparatus namely, microwave oven, television set, washing machine, refrigerator, compact fluorescent lamps (CFLs), high and low speed fans. These loads are connected to electrical outlets where voltage can be both 120 and $240V$. #AWG-14 cables are used for electrification of each unit, which has a rating of 15 A [35].

B. TRANSITION FROM GRID-CONNECTED MODE TO ISLANDED MODE

A residential unit may have access both grid power and local generation. Some loads are served by the utility power, others by DG units. The utility power can be used for heavier loads

such as washing machines, driers, and refrigerators. Lighter loads for example CFLs, fans, computers might be dedicated to the PV/battery hybrid system unit. To investigate system behaviors during a transition from a grid-connected mode to an islanded mode, bus#14 is simulated with a three-phase to ground fault, which is non-recoverable in a typical 5 cycles time period. The DG units in the residential microgrid (hybrid PV/battery system) will serve the loads under this scenario. The simulation results are presented in Figures 5 and 6.

Prior to $t_1 = 10s$, the grid is operating normally with the primary feeder operating at $f = 60Hz$ and $V_{rms} = 13.8kV$, as evident from the Fig.5(a). A zoomed-in version of the same figure is also shown, for visualization purposes. Fig.5(c), shows the DC power profile of the system. For the duration of the simulation run i.e. $75s$, it is assumed that the PV power generation is constant at $1000W$. This is represented by $P_{pv_{\phi_A}}$. The respective charging and discharging of the battery in the hybrid unit is represented by $P_{batt_{\phi_A}}$ and by the state-of-charge (SOC) in Fig.6(a). Since some of the loads in the residential microgrid will be supported by the grid and others by the PV/battery hybrid unit, the AC power profile in Fig.5(c) illustrates the contributions by the grid and the hybrid unit respectively.

At $t_1 = 10s$, an extended three-phase to ground fault is detected. At this point, the grid becomes unavailable. Hence, the total load is taken up by the hybrid unit, as shown in Fig.5(c). After $t_1 = 10s$, the load transitions are simulated by step changes of $144W$. At this stage, any additional PV power available will be used to charge the battery. This is illustrated between $t_1 = 10s$ and $t_2 = 20s$ in Fig.5(b). Between $t_2 = 20s$ and $t_3 = 65s$, both the PV and battery units contribute towards the loads. This is shown by the battery discharging in Fig.5(b) with the respective change in SOC in Fig.6(a). After $t_3 = 65s$ till the end of the simulation run, the battery starts charging again. This is because the loading deceases below the PV power. At this time, only the PV unit will serve the loads while the battery is being charged. Since the loading trajectories are such that the hybrid unit alone is capable of handling the loads, the droop unit is not required, as shown in Fig.5(c). The intra-phase power management scheme introduced in [20], [21] allows the system to operate between $f_{max} = 60.25Hz$ and $f_{min} = 59.95Hz$, as evident from Fig.6(b). Similar results can be obtained for other phases also.

From these simulation studies, it can be concluded that the benchmark distribution system is capable of operating both in grid-connected and islanded conditions. The system is also capable of coordinating a hybrid PV/battery unit with the local loads.

C. INTRA-PHASE POWER MANAGEMENT

The simulation results for intra-phase power management strategy are shown in Fig.7. The load increases in steps of $288W$. The simulation is run for $130s$, with step changes in loads after every $10s$. In this simulation run, it is assumed that ϕ_A is already operating in islanded condition. The battery has

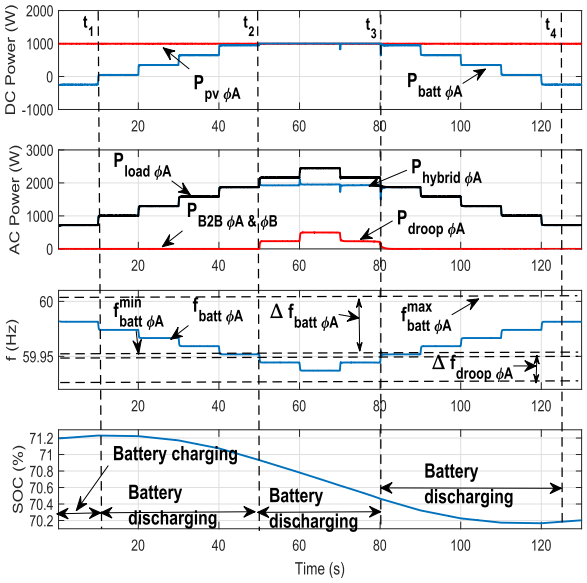

FIGURE 7. Performance of the intra-phase power management system.

an initial SOC of 71.2%. As a result of the relatively low load demand at early part of the simulation, the battery charges with the excess PV power generation in ϕ_B. The SOC control as shown in Fig.3, manages the battery to be charged till the maximum threshold of SOC_{max}. The charging state is evident from the negative battery power between $t_1 = 0s$ and $t_2 = 5s$. As per the operational scenario #1 in Table 1, the system frequency is the above nominal frequency, f_0, under islanded condition.

Further increase in the load demand between $t_2 = 5s$ and $t_3 = 10s$, causes the battery to be in the floating state as $P_{pv_{\phi_B}} = P_{load_{\phi_B}}$ i.e. $P_{batt_{\phi_B}} = 0W$. In this case, the total PV power is used to support the load. This validates scenario #2 in Table 1.

Between $t_3 = 10s$ and $t_4 = 25s$, the load increases further. In this case, the hybrid PV and battery units start supporting the load, as is represented by positive battery power, $P_{batt_{\phi_B}}$, in Fig.7. As per the improved multi-segment droop strategy, the system operates below the nominal frequency, f_0, [20], [21]. This validates scenario #3 in Table 1.

At $t_4 = 25s$, the battery unit is supplying its rated power of P_{batt}^{max}, with the system operating at f_{batt}^{min}. The SOC control block in Fig.3, will regulate the battery power at $1000W$, which is the capacity of the battery. Therefore, any increase in load demand will cause a power imbalance. For intra-phase power management strategy in the proposed benchmark distribution system, this power imbalance will be catered by the additional droop unit in the phase, represented by $P_{droop_{\phi_B}}$ in Fig.7. This validates scenario #4 in Table 1.

From $t_5 = 35s$ and $t_9 = 70s$, the load demand starts to decrease. Firstly, the contribution from the droop unit decreases to $0W$ and and then, the PV and battery units start supporting the load once again. As the load demand decreases below $P_{pv_{\phi_B}}$ at $t_8 = 60s$, the battery charging resumes. This is reflected in the increase of battery's SOC in Fig.7.

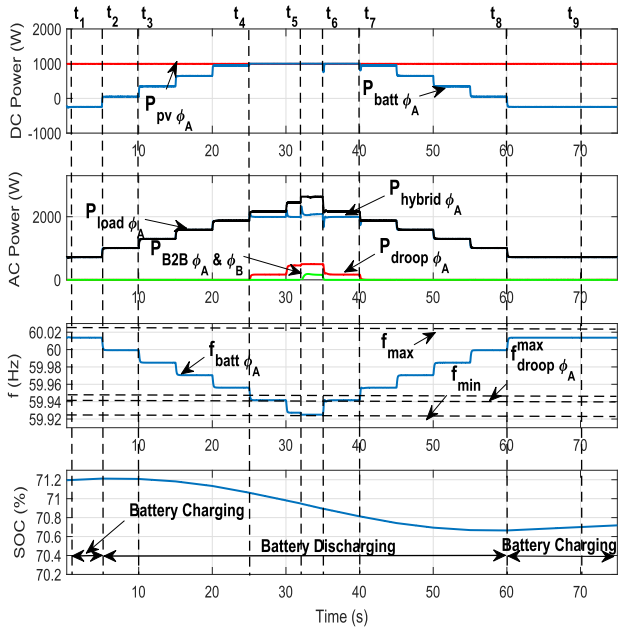

FIGURE 8. Performance of the inter-phase power management system.

Based on the results of these simulations, it can be concluded that the proposed intra-phase power management in the benchmark model is capable of coordinating multiple DG units effectively. This feature is crucial when dealing with single-phase DG and storage units in a distribution network.

D. INTER-PHASE POWER MANAGEMENT

The inter-phase power transfer can be observed at $t_5 = 32s$ in Fig.8. At this point, the PV, battery and droop units are already at their rated power output. Further increase in the load demand will cause power deficiency in ϕ_B. Thus, in order to maintain power balance in this phase, the proposed intra-phase power management strategy alone is no longer sufficient. In this case, inter-phase power management strategy is required to transfer the additional power from power-surplus phase to the power-deficient phase to maintain the system frequency at f_{min}. The inter-phase power transfer is initiated by the Local Energy Balance Control System and the respective logic, as shown in Fig.4, to activate the necessary back-to-back converter of ϕ_A. The signal $E_{B2B_{A,B,C}}$, as shown previously in Fig.4, are used for this purpose. The power reference for the back-to-back converter is communicated from the Local Energy Balance Control System to the Community Energy Balance Control System. For the simulated case as shown in Fig.8, ϕ_A supplies ϕ_B with the required net power. Similar results can be obtained for other phases also. Further details on this control strategy can be found in [20], [21].

The simulation results have demonstrated that, by inclusion of an inter-phase power management unit, the developed benchmark distribution system model is capable of dealing with and mitigating system imbalance due to single-phase DG, storage units, and load.

VII. CONCLUSION

A new benchmark distribution system model capable of supporting studies of residential microgrids has been developed. This model supports both grid-connected and islanded systems, as well as transitions from one to the other. A unique feature of this model is that it allows for integration of multiple single-phase DG sources to be located in a particular phase, yet, it also supports coordination of these units within their respective phases or across different phases. This is accomplished by an intra-phase power management and an inter-phase power management units. This proposed benchmark model will allow utility personnel to investigate the impact of ever increasing installation of roof-top PV units and residential energy storage units. Introduction of the intra-phase and the inter-phase power management units improves controllability of the distribution system significantly for load balancing within a single phase or among three phases, when the DG and storage units are operating indiscriminately. Three case studies have been carried out using this newly developed benchmark to illustrate its effectiveness.

APPENDIX

The CIEMAT charging model of a lead acid battery is given by [29],

$$V_{Charge}(t) = [2 - 0.16SOC(t)] + \frac{i_B(t)}{C_B}\left(\frac{6}{1 + i_B(t)^{0.86}} + \frac{0.48}{(1 - SOC(t))^{1.2}} + 0.036\right) \times (1 - 0.025\Delta T) \quad \text{(A.1)}$$

where, C_B, i_B and V_{Charge} are the capacity, charging current, and voltage of the battery respectively. The SOC is calculated using,

$$SOC(t) = \frac{1}{C_B \times 3600}\left[\int_0^{\tau} i_B(t)\ dt\right] \times 100\% \quad \text{(A.2)}$$

where, τ is the time constant. The discharge model of battery is given by,

$$V_{Discharge}(t) = [2.085 - 0.12(1 - SOC(t))] - \frac{i_B(t)}{C_B}\left(\frac{4}{1 + i_B(t)^{1.3}} + \frac{0.27}{SOC(t)^{1.5}} + 0.02\right) \times (1 - 0.007\Delta T) \quad \text{(A.3)}$$

ACKNOWLEDGMENT

The authors would like to thank the local utility, London Hydro, for providing useful information on the practical distribution systems upon which this study is based.

REFERENCES

[1] ARUP. *Five Minute Guide to Rooftop Solar PV*. Accessed: Apr. 20, 2019. [Online]. Available: https://www.arup.com/perspectives/publications/promotional-materials/section/five-minute-guide-to-rooftop-solar-pv

[2] R. Majumder, "Aggregation of microgrids with DC system," *Electr. Power Syst. Res.*, vol. 108, pp. 134–143, Mar. 2014.

[3] L. Che, M. Shahidehpour, A. Alabdulwahab, and Y. Al-Turki, "Hierarchical coordination of a community microgrid with AC and DC microgrids," *IEEE Trans. Smart Grid*, vol. 6, no. 6, pp. 3042–3051, Nov. 2015.

[4] L. G. Meegahapola, D. Robinson, A. P. Agalgaonkar, S. Perera, and P. Ciufo, "Microgrids of commercial buildings: Strategies to manage mode transfer from grid connected to islanded mode," *IEEE Trans. Sustain. Energy*, vol. 5, no. 4, pp. 1337–1347, Oct. 2014.
[5] A. Mehrizi-Sani and R. Iravani, "Potential-function based control of a microgrid in islanded and grid-connected modes," *IEEE Trans. Power Syst.*, vol. 25, no. 4, pp. 1883–1891, Nov. 2010.
[6] G. T. Heydt, "The next generation of power distribution systems," *IEEE Trans. Smart Grid*, vol. 1, no. 3, pp. 225–235, Dec. 2010.
[7] F. Han, X. Yu, Y. Wang, and M. Al-Dabbagh, "Sinusoidal steady-state analysis for fault location in power distribution systems," in *Proc. 30th Annu. Conf. IEEE Ind. Electron. Soc. (IECON)*, vol. 3, Nov. 2004, pp. 3014–3018.
[8] L. Xiao, Z. Xu, T. An, and Z. Bian, "Improved analytical model for the study of steady state performance of droop-controlled VSC-MTDC systems," *IEEE Trans. Power Syst.*, vol. 32, no. 3, pp. 2083–2093, May 2017.
[9] H. P. Schmidt, N. Ida, N. Kagan, and J. C. Guaraldo, "Fast reconfiguration of distribution systems considering loss minimization," *IEEE Trans. Power Syst.*, vol. 20, no. 3, pp. 1311–1319, Aug. 2005.
[10] S. S. Khorramabadi and A. Bakhshai, "Intelligent control of grid-connected microgrids: An adaptive critic-based approach," *IEEE J. Emerg. Sel. Topics Power Electron.*, vol. 3, no. 2, pp. 493–504, Jun. 2015.
[11] T. L. Vandoorn, J. C. Vásquez, J. De Kooning, J. M. Guerrero, and L. Vandevelde, "Microgrids: Hierarchical control and an overview of the control and reserve management strategies," *IEEE Ind. Electron. Mag.*, vol. 7, no. 4, pp. 42–55, Dec. 2013.
[12] H. R. Baghaee, M. Mirsalim, G. B. Gharehpetian, and H. A. Talebi, "Three-phase AC/DC power-flow for balanced/unbalanced microgrids including wind/solar, droop-controlled and electronically-coupled distributed energy resources using radial basis function neural networks," *IET Power Electron.*, vol. 10, no. 3, pp. 313–328, 2017.
[13] A. La Bella, S. R. Cominesi, C. Sandroni, and R. Scattolini, "Hierarchical predictive control of microgrids in islanded operation," *IEEE Trans. Autom. Sci. Eng.*, vol. 14, no. 2, pp. 536–546, Apr. 2017.
[14] P. Tenti, A. Costabeber, F. Sichirollo, and P. Mattavelli, "Minimum loss control of low-voltage residential microgrids," in *Proc. 38th Annu. Conf. IEEE Ind. Electron. Soc. (IECON)*, Oct. 2012, pp. 5650–5656.
[15] Z. Xu, P. Yang, Y. Zhang, T. He, J. Peng, and Q. Zheng, "Control devices development of residential single-phase PV-ESS microgrid," in *Proc. IEEE Innov. Smart Grid Technol.-Asia (ISGT-Asia)*. Nov./Dec. 2016, pp. 914–919.
[16] A. C. Luna, N. L. Diaz, M. Graells, J. C. Vasquez, and J. M. Guerrero, "Cooperative energy management for a cluster of households prosumers," *IEEE Trans. Consum. Electron.*, vol. 62, no. 3, pp. 235–242, Aug. 2016.
[17] Q. Sun, J. Zhou, J. M. Guerrero, and H. Zhang, "Hybrid three-phase/single-phase microgrid architecture with power management capabilities," *IEEE Trans. Power Electron.*, vol. 30, no. 10, pp. 5964–5977, Oct. 2015.
[18] T. Gonen, *Electric Power Distribution Engineering*, 2nd ed. New York, NY, USA: Taylor & Francis, 2007.
[19] S. Freitas, T. Santos, and M. C. Brito, "Impact of large scale PV deployment in the sizing of urban distribution transformers," *Renew. Energy*, vol. 119, pp. 767–776, Apr. 2018.
[20] S. A. R. Naqvi and J. Jiang, "Cooperative control and power management for islanded residential microgrids with local phase-wise generation and storage units," in *Proc. 7th Int. Conf. Renew. Energy Res. Appl.*, 2018, pp. 239–244.
[21] S. A. Raza and J. Jiang, "Intra- and inter-phase power management and control of a residential microgrid at the distribution level," *IEEE Trans. Smart Grid*, vol. 10, no. 6, pp. 6839–6848, Nov. 2019.
[22] A. Hintz, U. R. Prasanna, and K. Rajashekara, "Comparative study of the three-phase grid-connected inverter sharing unbalanced three-phase and/or single-phase systems," *IEEE Trans. Ind. Appl.*, vol. 52, no. 6, pp. 5156–5164, Nov./Dec. 2016.
[23] R. Zhang, D. Boroyevich, V. H. Prasad, H.-C. Mao, F. C. Lee, and S. Dubovsky, "A three-phase inverter with a neutral leg with space vector modulation," in *Proc. Appl. Power Electron. Conf. (APEC)*, vol. 2, Feb. 1997, pp. 857–863.
[24] P. Verdelho and G. D. Marques, "Four-wire current-regulated PWM voltage converter," *IEEE Trans. Ind. Electron.*, vol. 45, no. 5, pp. 761–770, Oct. 1998.
[25] Y. Li, D. M. Vilathgamuwa, and P. C. Loh, "Microgrid power quality enhancement using a three-phase four-wire grid-interfacing compensator," *IEEE Trans. Ind. Appl.*, vol. 41, no. 6, pp. 1707–1719, Nov. 2005.
[26] R. R. Sawant and M. C. Chandorkar, "A multifunctional four-leg grid-connected compensator," *IEEE Trans. Ind. Appl.*, vol. 45, no. 1, pp. 249–259, Jan. 2009.
[27] V. Khadkikar and A. Chandra, "An independent control approach for three-phase four-wire shunt active filter based on three H-bridge topology under unbalanced load conditions," in *Proc. IEEE Power Electron. Spec. Conf.*, Jun. 2008, pp. 4643–4649.
[28] C. L. Chen, C. E. Lin, and C. L. Huang, "An active filter for unbalanced three-phase system using synchronous detection method," in *Proc. IEEE Power Electron. Spec. Conf. (PESC)*, Jun. 1994, pp. 1451–1455.
[29] N. Achaibou, M. Haddadi, and A. Malek, "Lead acid batteries simulation including experimental validation," *J. Power Sources*, vol. 185, no. 2, pp. 1484–1491, 2008.
[30] Ontario Distribution Review Panel. (2012). *Renewing Ontario's Electricity Distribution Sector: Putting the Customer First*. Accessed: Apr. 20, 2019. [Online]. Available: http://www.energy.gov.on.ca/en/files/2012/05/LDC_en.pdf
[31] *IEEE Recommended Practice for Electric Power Distribution for Industrial Plants*, IEEE Standard 141-1993, 2nd ed., Institute of Electrical and Electronics Engineers, 1990.
[32] J. Burke. (2006). *Hard To Find Information About Distribution Systems*. Accessed: Apr. 20, 2019. [Online]. Available: https://library.e.abb.com/public/91ad3a29a50978bf85256c550053db0d/Hard.To.Find.6th.pdf
[33] Daycounter, Inc. *AWG-American Wire Gauge*. Accessed: Apr. 20, 2019. [Online]. Available: https://www.daycounter.com/Calculators/AWG.phtml
[34] H. N. Holzman, *Modern Residential Wiring*, 10th ed. Homewood, IL, USA: Goodheart-Willcox, 2014.
[35] M. J. Ghorbani, M. S. Rad, H. Mokhtari, M. E. Honarmand, and M. Youhannaie, "Residential loads modeling by Norton equivalent model of household loads," in *Proc. Asia–Pacific Power Energy Eng. Conf. (APPEEC)*, 2011, pp. 1–4.

SYED A. RAZA (S'14) received the bachelor's degree in electronics engineering from the National University of Science and Technology-School of Electrical Engineering and Computer Sciences (NUST-SEECS), Pakistan, in 2009, and the master's degree in electrical engineering from the King Fahd University of Petroleum and Minerals, Saudi Arabia, in 2012. He is currently pursuing the Ph.D. degree with The University of Western Ontario, Canada.

From 2012 to 2014, he was an Instructor with the Department of Electrical Engineering, Prince Mohammad Bin Fahd University. He is a member of the Distributed Generation Laboratory, The University of Western Ontario. His main areas of research include power management strategies for PV/battery-based residential microgrids, the dynamical control of power systems, and the applications of system identication techniques in non-linear systems. He was a recipient of the London Hydro Scholarship, in 2015.

JIN JIANG (S'85–M'87–SM'94–F'17) received the Ph.D. degree from the University of New Brunswick, Fredericton, NB, Canada, in 1989.

Since 1991, he has been with the Department of Electrical and Computer Engineering, The University of Western Ontario, London, ON, Canada, where he is currently a Distinguished University Professor and a Senior Industrial Research Chair Professor. His research interests include the fault-tolerant control of safety-critical systems, the advanced control of electrical power plants, and power systems, especially microgrids involving renewable energy resources.

Dr. Jiang is a Fellow of the Canadian Academy of Engineering. He is also a member of the International Electrotechnical Commission 45A subcommittee to develop industrial standards on instrumentation and control for nuclear facilities. He also works closely with the International Atomic Energy Agency on modern control and instrumentation for nuclear power plants.